Catalysis
Science & Technology

RSC Publishing

PAPER

View Article Online
View Journal

Published on 07 October 2013. Downloaded by Memorial University of Newfoundland on 10/11/2013 16:34:56.

Cite this: DOI: 10.1039/c3cy00691c

Isopropylation of naphthalene by isopropanol over conventional and Zn- and Fe-modified USY zeolites†

Marimuthu Banu,‡[a] Young Hye Lee,‡[b] Ganesan Magesh[a] and Jae Sung Lee*[a]

Received 10th September 2013,
Accepted 5th October 2013

DOI: 10.1039/c3cy00691c

www.rsc.org/catalysis

Catalytic performances of USY, MOR, and BEA zeolites were compared for the isopropylation of naphthalene by isopropyl alcohol in a high-pressure, fixed-bed reactor. The USY catalyst showed a high conversion of 86% and good stability but a low 2,6-/2,7-DIPN shape selectivity ratio of 0.94. In contrast, over the MOR catalyst, 2,6-DIPN was selectively synthesized with a high 2,6-/2,7-DIPN ratio of 1.75, but low naphthalene conversions and fast deactivation of the catalyst were observed. The USY catalyst was modified by Zn and Fe using the wet impregnation method to enhance the selectivity for 2,6-DIPN. The highest conversion (~95%) and selectivity for 2,6-DIPN (~20%) were achieved with 4% Zn/USY catalyst. It appeared that small metal oxide islands formed in the USY pores to decrease the effective pore size and thus render it mildly shape-selective. Zn loading also decreased the number of strong acid sites responsible for coke formation and increased the number of weak acid sites. The high conversion and stability of Zn-modified catalysts were ascribed to the presence of a suitable admixture of weak and strong acid sites with less coke deposition. The Fe-modified USY catalysts were less effective because the modification increased the number of the strong acid sites.

1. Introduction

2,6-Dialkylnaphthalene (2,6-DAN) is a key intermediate for manufacturing polyethylene naphthalate (PEN), a high performance thermoplastic polyester. Alkylation of naphthalene is a route to produce 2,6-DAN using various alkylating agents, such as methanol, ethanol, isopropyl alcohol, propene, isopropyl bromide and cyclohexene.[1–8] Among several routes, isopropylation using isopropanol attracts more attention due to the presence of a more sterically hindered isopropyl group, which provides a high possibility of the selective synthesis of 2,6-diisopropylnaphthalene (2,6-DIPN) in a suitable intracrystalline channel of zeolite. Zeolites are well known as shape selective catalysts for naphthalene isopropylation that obtain 2,6-DIPN selectively due to their unique pore dimensions and optimum acidic sites.[9]

Katayama *et al.* obtained a higher selectivity for 2,6-DIPN (52%) over the H-MOR catalyst than over H-Y, H-L and H-ZSM-5 catalysts.[3] Kim *et al.* carried out isopropylation of naphthalene over the dealuminated H-mordenite catalyst and concluded that the reaction occurred at the acid sites in pore entrances, leading to enhanced selectivity for the 2,6-DIPN product with minimum coke deposition.[5] Similar results have been reported by many other researchers.[6,10–12] On the other hand, some studies reported high 2,6/2,7-DIPN shape selectivity ratios over the H-Y zeolite catalyst as well.[13–16] There have been efforts to improve the performance by modification of zeolites. Thus, Kamalakar *et al.* carried out naphthalene ethylation using ethanol over La, Ce, and Mg cation-modified H–Y zeolites and observed a high conversion of 57.2% and a selectivity of 31.3% for 2,6-diethylnaphthalene (2,6-DEN) over Ce (5 wt%)- and Mg (3 wt%)-Y catalysts. They also studied the same reaction over Ce, Fe or K-modified HY, HMCM-41 and SAPO-5 zeolite catalysts and observed high selectivities for 2,6-DEN over CeKY (25.2%) and FeY (20.4%) catalysts.[2,17] Kang *et al.* studied the isopropylation of naphthalene by a cation (Zn^{2+}, Co^{2+}, Ca^{2+} or Mg^{2+})-exchanged Y-zeolite, in which the cation improved the stability by forming less coke, but selectivity for 2,6-DIPN was not improved.[18] Recently, Hajimirzaee *et al.* modified the H-Y zeolite with transition metals such as Fe, Co, Ni and Cu for the naphthalene isopropylation reaction and observed a high 2,6/2,7 shape selectivity ratio of 6.6 over the Fe/HY catalyst.[19] Although there is some inconsistency in the reported data, it is clear that the activity, selectivity, and stability of the isopropylation of naphthalene could be improved by suitable modification of zeolite catalysts.

Herein, we studied the catalytic activity, selectivity and stability of pore-modified USY zeolite catalysts in the isopropylation of naphthalene using isopropanol. Pores were modified by the

[a] *School of Energy and Chemical Engineering, Ulsan National Institute of Science and Technology (UNIST), Ulsan, Korea. E-mail: jlee1234@unist.ac.kr; Fax: +82 52 217 1019; Tel: +82 52 217 2544*

[b] *Department of Chemical Engineering, Pohang University of Science and Technology (POSTECH), Pohang, Korea*

† Electronic supplementary information (ESI) available. See DOI: 10.1039/c3cy00691c

‡ These authors contributed equally.

Published on 07 October 2013. Downloaded by Memorial University of Newfoundland on 10/11/2013 16:34:56.

impregnation of Zn and Fe, which changed the effective pore size and acid strength of the USY zeolite. The influence of the metal loading of Zn (2, 4, 6, 8 wt%) or Fe (2, 4, 6 wt%) onto the USY zeolite on naphthalene conversion and selectivity for 2,6-DIPN was studied. A detailed analysis of the isomeric distributions of IPN (monoisopropylnaphthalenes) and DIPN was carried out over different catalysts. As a key parameter representing shape selectivity, the 2,6/2,7-DIPN ratio was monitored. Among all catalysts studied, 4% Zn/USY catalyst exhibited the highest conversion (~95%) and selectivity for 2,6-DIPN (~20%), which represents a significant improvement over unmodified USY (86% and 17%).

2. Experimental

2.1. Catalyst synthesis

USY (CBV780, SiO_2/Al_2O_3 = 80), NH_3-BEA (CP814E, SiO_2/Al_2O_3 = 25), and Na-MOR (CBV10A, SiO_2/Al_2O_3 = 25), all from Zeolyst, were used as parent alkylation catalysts. The acid form of zeolite beta was generated by calcination of NH_4^+-BEA at 500 °C for 5 h in air. H-MOR was prepared by the repeated ion exchange of Na-MOR with 1 M NH_4NO_3 solution at 80 °C followed by drying overnight at 80 °C and calcination at 550 °C for 5 h in air. Zn or Fe was loaded onto the USY zeolite by an incipient wetness method using different amounts of $Zn(NO_3)_2{\cdot}6H_2O$ or $Fe(NO_3)_2{\cdot}6H_2O$ in aqueous solution to obtain catalysts with the desired loading of Zn (2, 4, 6 and 8 wt%) or Fe (2, 4 and 6 wt%). The Zn- and Fe-loaded samples were dried at 120 °C for 12 h followed by calcination at 500 °C for 5 h in air.

2.2. Catalyst characterization

Powder X-ray diffraction (XRD) patterns were obtained using a PW3040/60 Xpert PRO (PANalytical) with Cu Kα radiation. The chemical compositions of the samples were measured using an ICP spectrometer (Jobin Yuon, model JY-38 VHR). The surface area and pore volume of the samples were obtained from N_2 sorption isotherms (Nanoporosity XQ Analyser). ^{27}Al NMR spectra were recorded at room temperature using a VNMRS 600 NB spectrometer (14.1 T) at a spin rate of 15 kHz. A resonance frequency of 156.3 MHz, a recycle delay of 0.5 s and 7000 scans were applied. The morphology was determined using an FE-SEM XL30S FEG Philips scanning electron microscope. Temperature-programmed desorption (TPD) of ammonia was carried out to probe the distribution of acidity in the prepared catalyst. The HRTEM images were recorded on a JEOL JEM-2100F/CESCOR microscope operated at 200 kV. The amount of coke deposited on the catalysts was calculated by a temperature-programmed oxidation (TPO) analysis (Micromeritics Auto Chem II) of the used catalysts.

2.3. Isopropylation of naphthalene using isopropanol

All of the catalytic experiments were carried out in a continuous, high-pressure fixed-bed reactor with an inner diameter of 1/2 inch. A reactant mixture of naphthalene and isopropyl alcohol dissolved in decalin was injected through a high pressure pump into a tubular stainless-steel reactor, the middle of which was loaded with 1.0 g of catalyst in the form of granules (20–40 mesh). A thermocouple placed close to the catalyst bed was used to measure the reaction temperature. Before the start of the reaction run, the catalyst was activated *in situ* in N_2 flow at 550 °C for 4 h to drive off moisture and adsorbed hydrocarbons, if any. The typical reaction conditions were as follows: temperature, 250 °C; pressure, 3.0 MPa; weight hourly space velocity (WHSV, total liquid feed), 3 h^{-1}; time on stream (TOS), 8 h; molar ratio of naphthalene, isopropyl alcohol, and decalin in liquid feed, 1 : 2 : 7.5. To keep the system at a steady high pressure, 10 ml min^{-1} of N_2 was introduced into the reactor along with the reaction feed. The reactor effluent was condensed in the sampler and sampled hourly. The products were analyzed by GC (model HP 7890) using an FID detector furnished with a 60 m × 0.25 mm × 0.25 μm (HP INNOWAX) capillary column. The analytical conditions were as follows: flow rate of H_2 (carrier gas) in the column, 1.5818 ml min^{-1}; split ratio, 100; detector temperature, 300 °C; injection temperature, 300 °C. The temperature program of the column started at an initial temperature of 120 °C for 3 min followed by a temperature ramp of 8 °C min^{-1} and a final temperature of 220 °C for 30 min.

3. Results and discussions

3.1. Catalytic isopropylation of naphthalene over conventional zeolites

The isopropylation of naphthalene produces a number of products depending on the substitution of the isopropyl group at the α or β positions of naphthalene. As presented in Scheme 1, the possible products are α,α-(1,4-; 1,5-), α,β-(1,6-; 1,3-; 1,7-) and β,β-(2,6-; 2,7-), and their sizes decrease in the order α,α > α,β > β,β. 2,6-DIPN and 2,7-DIPN are the slimmest products

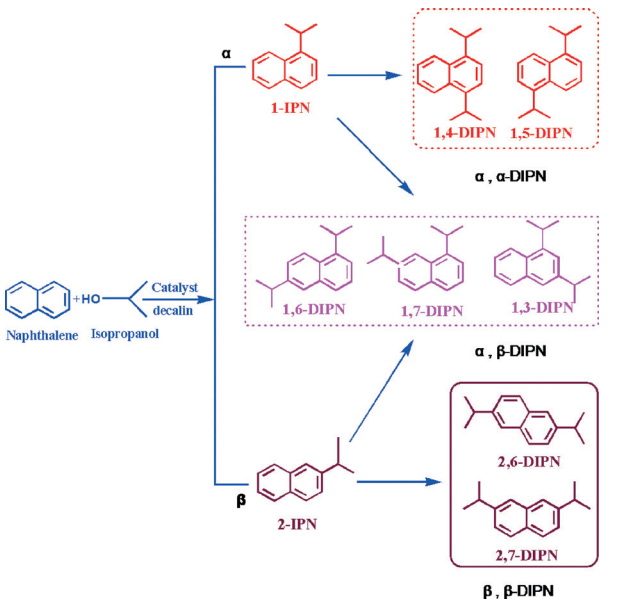

Scheme 1 Possible product distributions for isopropylation of naphthalene.

This journal is © The Royal Society of Chemistry 2013

Published on 07 October 2013. Downloaded by Memorial University of Newfoundland on 10/11/2013 16:34:56.

with dimensions of 0.661 × 0.661 × 1.423 nm and 0.662 × 0.726 × 1.376 nm, respectively. The separation of the isomers is difficult, and thus a high 2,6/2,7-DIPN ratio in the reaction products is particularly desired.

First, we studied naphthalene isopropylation over commercial USY, MOR and BEA zeolite catalysts at 250 °C, 3.0 MPa and a WHSV of 3 h^{-1} to study the effects of zeolite structure. As shown in Table 1, USY catalysts showed a high naphthalene conversion of 86%, whereas the MOR and BEA catalysts showed naphthalene conversions of ~54% and ~77%, respectively. After 6 h of continuous reaction, the conversion followed the same order: USY (86.2%) > BEA (76.8%) > MOR (53.7%). Over the MOR catalyst, the major product was monoalkylated IPN (73%), and DIPN selectivity was 26% with no polyisopropylnaphthalene (PIPN) products. In the case of the USY catalyst, DIPN was observed as the major product with ~52% selectivity, while IPN and PIPN selectivities were 39% and 6%, respectively. The BEA zeolite catalyst showed IPN, DIPN and PIPN product selectivities of 51%, 38% and ~11%, respectively. The 2,6-DIPN selectivity after 6 h on stream was in the order MOR (8%) < BEA (11%) < USY (17%). The 2,6/2,7-DIPN shape selectivity ratios varied as: MOR (1.75) > BEA (1.22) > USY (0.94). This trend of activity and selectivity was consistent with the pore size of the zeolites. Thus USY with the largest pores showed the highest conversion and the highest selectivity for the desired 2,6-DIPN, which is one of the thermodynamically most stable products. But the 2,6/2,7-DIPN shape selectivity ratio was the lowest because of the absence of spatial constraint.

The stability of the catalysts could be investigated by monitoring the changes in the time on stream in naphthalene conversions, selectivity for 2,6-DIPN and the ratio of 2,6-/2,7-DIPN as presented in Fig. 1. The results show that catalyst stability increases as MOR < BEA < USY. The trend also reflects the pore size and structure of the zeolites in agreement with earlier reports.[14,20–23] The MOR zeolite has a one dimensional pore channel with a 12-membered ring size of 0.65 × 0.70 nm. The BEA zeolite has a larger 12-membered ring pore channel of 0.64 × 0.76 nm.[22] The USY zeolite has three dimensional pore channels with a 12-membered ring size of 0.74 nm, which connect large super cages of 1.3 nm. Since 2,6-DIPN has a similar size to the window size of MOR, it leads to a high 2,6/2,7-DIPN ratio. Deactivation occurs over MOR owing to the large amount of coke from polynuclear cracking in the pore mouth, which blocks access by the reactant molecules. The large pore size of USY does not allow any shape selectivity. Instead, pores are easily accessed by reactant molecules, and the chance of pore blocking by coke is minimal. It shows the highest selectivity for 2,6-DIPN because 2,6- and 2,7-DIPN are thermodynamically the most stable products among DIPNs.

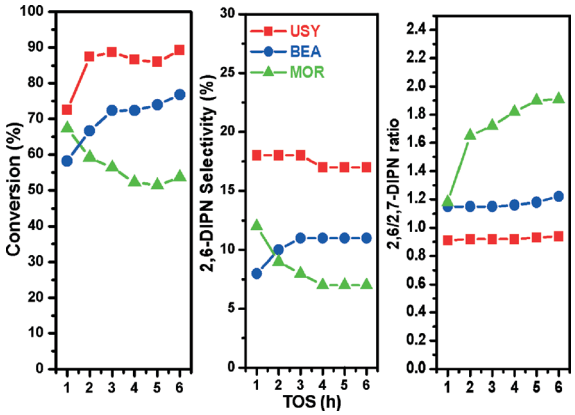

Fig. 1 Conversion, 2,6-DIPN selectivity and 2,6/2,7-DIPN ratio for naphthalene isopropylation over commercial zeolite catalysts. Reaction conditions: T = 250 °C; P = 30 bar; WHSV = 3 h^{-1}; isopropanol/naphthalene/decalin molar ratio: 1 : 2 : 7.5.

3.2. Modification of USY zeolite by Zn and Fe

Among the three zeolites studied, USY provided the highest naphthalene conversion, selectivity for 2,6-DIPN, and stability. Yet, the shape selectivity represented by the 2,6/2,7-DIPN ratio was the lowest. We attempted to improve the performance of USY by modification of its pores. The pore structures of zeolites could be modified by various methods such as desilication, dealumination and metal loading.[24,25] Thus we have modified the USY pores by loading Zn and Fe oxides, which are also known as promising catalysts for alkylation and acylation reactions.[26]

The XRD patterns of Zn (2–8 wt%)-loaded USY catalysts show the characteristic peak of the ZnO (100) plane in addition to the peaks of the USY zeolite with a high loading of Zn/USY (6, 8 wt%) as presented in Fig. 2. There was no characteristic peak observed in Fe (2–6%)/USY catalysts (not shown) due to their high dispersion into the channel of the USY zeolite.[27] It is expected that ZnO and Fe_2O_3 will form under the calcination conditions employed here.

The N_2 adsorption–desorption isotherms (Fig. S1†) of USY and metal-loaded USY catalysts show the type I isotherms

Table 1 Isopropylation of naphthalene over commercial zeolites[a]

Catalyst	Conv. (%)	Selectivity (%)				2,6-DIPN yield[b]	2,6/2,7 ratio
		IPN	DIPN	PIPN	2,6-DIPN		
USY	86.2	39.1	51.6	6.2	17	16.1	0.94
MOR	53.7	73.6	26.4	0	8	4	1.75
BEA	76.8	51.5	38.0	10.5	11	8.5	1.22

[a] T = 250 °C, P = 30 bar, WHSV = 3 h^{-1}, TOS = 6 h and isopropanol/naphthalene/decalin molar ratio = 1 : 2 : 7.5. [b] Naphthalene conversion × 2,6-DIPN selectivity.

Published on 07 October 2013. Downloaded by Memorial University of Newfoundland on 10/11/2013 16:34:56.

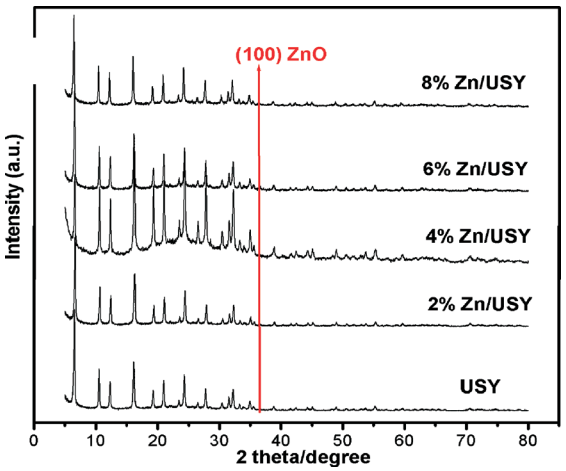

Fig. 2 XRD patterns of Zn-loaded USY catalysts. The presence of the ZnO (100) peak could be noted in 6 and 8 wt% Zn/USY.

which indicate that the zeolite texture remains intact upon incorporation of Zn and Fe ions. Moreover, it is noteworthy that at high relative pressures, a hysteresis loop appears due to capillary condensation, which is generally associated with the creation of mesopores.[28] The point where the adsorption and desorption branches of the isotherm meet represents the critical diameter of pores causing capillary condensation. The point slightly shifted from a P/P_0 of 0.40 to a P/P_0 of 0.44 over 2–4% Zn/USY catalysts (decreased pore size), confirming the metal oxides growing inside the micropores during calcination. Over 6–8% Zn/USY catalysts, it returns to its original value of 0.40, which can be attributed to the blocking of the pore mouth due to the presence of a large amount of metal oxides.[29] A similar trend has also been observed on Fe-loaded USY catalysts.

The textural properties derived from the N_2 adsorption isotherms are summarized in Table 2, including BET surface area, micropore area, micropore volume and mean micropore diameter for all of the prepared catalysts.

The total BET surface area and micropore area observed on the parent USY were 773 $m^2\ g^{-1}$ and 608 $m^2\ g^{-1}$, respectively. The mean micropore diameter was calculated using the *t*-plot method. The micropore volume and mean micropore diameter of USY were 0.27 $cm^3\ g^{-1}$ and 9.01 Å, respectively.

The BET surface area and micropore area decreased after metal loading, except for the 2% Fe/USY catalyst that showed a slight increase in BET area. The pore volume remained similar with Fe loading, while it decreased after Zn loading as reported in earlier works.[19,30–32] The mean micropore diameter decreased a little to 8.99 Å, 8.88 Å and 8.99 Å on 2%, 4% and 6% Zn/USY catalysts, respectively. In contrast, it increased from 9.01 Å to 9.08 Å on 8% Zn/USY catalyst. In the case of Fe-loaded USY catalysts, the mean micropore diameter decreased consistently from 9.01 Å to 8.99, 8.96 and 8.85 Å on 2%, 4% and 6% Fe/USY catalysts, respectively. A similar result has been observed for HK pore size distributions in Fig. S2† as well.

^{27}Al NMR was used to probe any change in the Al environment depending on the catalyst treatments, and the spectra of Zn- and Fe-modified catalysts are given in Fig. 3. The ^{27}Al NMR spectrum of the parent USY showed four peaks centered at 3 ppm, 62 ppm, 35 ppm, and 15–20 ppm. The peaks at 3 ppm and 62 ppm correspond to the octahedrally and tetrahedrally coordinated Al species, respectively. Between them are two more peaks at 35 ppm and 15–20 ppm, corresponding to five-coordinated (or distorted tetrahedral) Al species and distorted octahedral Al species.[33,34] The Fe-loaded USY catalysts did not show any changes in the Al environment, but the Zn-loaded USY catalysts showed a slight decrease in the peaks

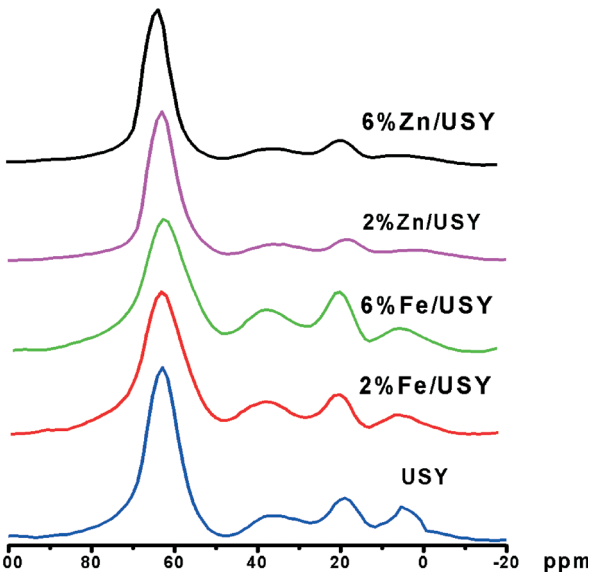

Fig. 3 ^{27}Al NMR spectra of Zn- and Fe-modified USY catalysts.

Table 2 Textural properties of the catalysts

Samples	Surface area ($m^2\ g^{-1}$)			Pore volume[a] ($cm^3\ g^{-1}$)	Mean micropore diameter[a] (Å)
	BET	Micropore[a]	External surface area[b]		
USY	773	608	165	0.27	9.01
2% Zn/USY	762	590	172	0.27	8.99
4% Zn/USY	658	492	166	0.22	8.88
6% Zn/USY	643	484	159	0.22	8.99
8% Zn/USY	643	474	169	0.22	9.08
2% Fe/USY	787	582	205	0.26	8.99
4% Fe/USY	746	577	169	0.26	8.96
6% Fe/USY	714	566	148	0.25	8.85

[a] Based on the *t*-plot method. [b] BET surface area − micropore area.

This journal is © The Royal Society of Chemistry 2013

Published on 07 October 2013. Downloaded by Memorial University of Newfoundland on 10/11/2013 16:34:56.

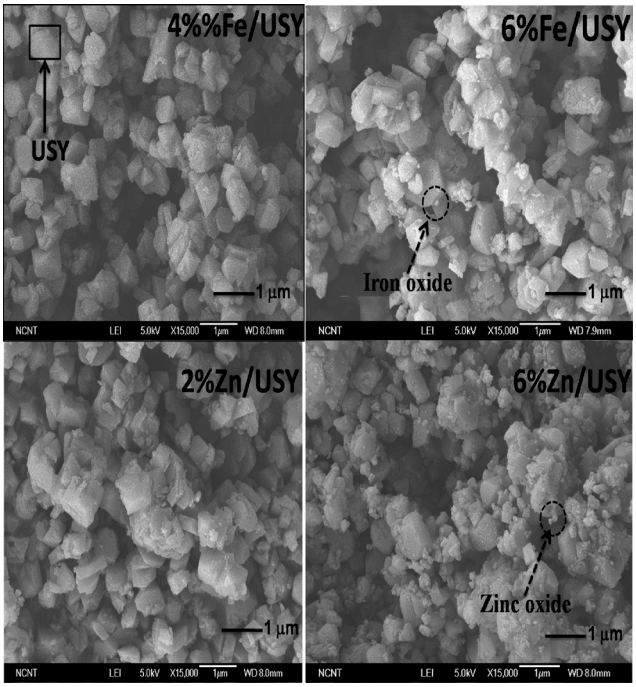

Fig. 4 SEM images of Zn- and Fe-loaded USY catalysts.

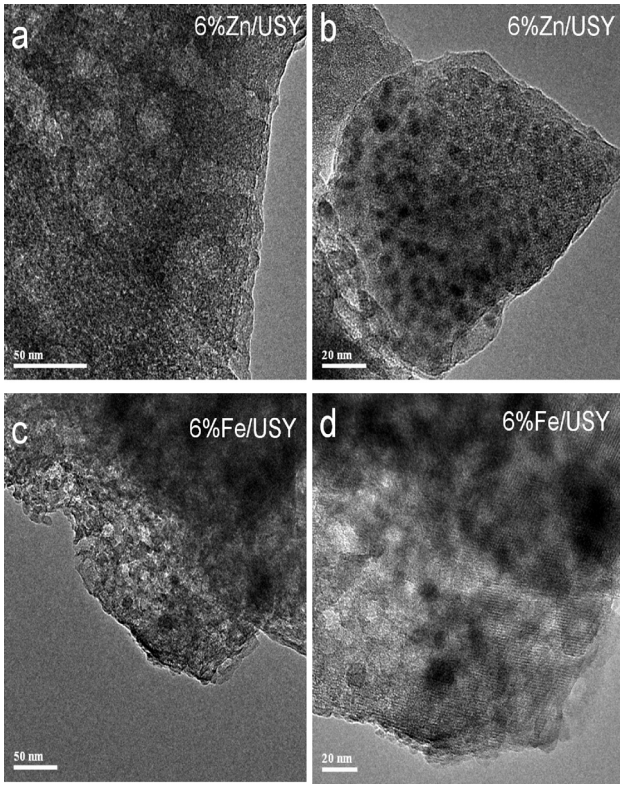

Fig. 5 HRTEM images of Zn (6%) and Fe (6%)-loaded USY catalysts.

at 3 ppm and 35 ppm. The results confirm that Zn or Fe loading does not affect the structure and the coordination environment of the USY framework.

The morphology of the external surfaces of the parent and modified USY was examined by SEM as shown in Fig. 4. No significant changes are observed for 2% Zn/USY and 4% Fe/USY catalysts, whereas there are many tiny metal oxide particles in 6% Zn/USY catalyst. The 6% Fe/USY catalyst exhibits relatively fewer metal oxide particles. The observation is also consistent with the metal oxides growing inside the micropores during calcination. The HRTEM technique was used to find out the distribution of Zn and Fe oxide particles on USY for high loading catalysts. As shown in Fig. 5, both Zn (6%)- and Fe (6%)-loaded USY catalysts showed well dispersed metal oxide particles on the surface of USY.

In Table 3, the Si/Al ratio of the parent USY is 47 from ICP analysis, and it remained similar in all of the metal-loaded USY catalysts. Thus metal oxide loading by impregnation does not affect the USY zeolite itself as confirmed by ^{27}Al NMR analysis in Fig. 3. The relative acid strength distributions in the parent and modified USY catalysts were determined by temperature-programmed desorption (TPD) of NH_3 in the temperature range of 80–800 °C, and the results are presented also in Table 3. The temperature of NH_3 desorption represents the strength of the acid sites of the zeolites.[35] Desorption below 100 °C is due to physisorbed NH_3, but it is not observed in our samples. Desorption at 100–350 °C is attributed to weak acid sites due to the presence of trivalent aluminum in the zeolite framework. Desorption above 350 °C is due to the strong acidic sites. The weak, strong and total acidic sites on the parent USY are 0.125 mmol g^{-1}, 0.148 mmol g^{-1} and 0.273 mmol g^{-1}, respectively. There is a significant decrease in strong acidity

Table 3 Acidity based on NH_3-TPD, chemical composition of the prepared catalysts and the amount of coke deposited on the used catalysts according to TGA analysis

	Concentration of acid sites (mmol g^{-1})				
	Weak	Strong		Si/	Amount of coke formed
Samples	100–350 °C	>350 °C	Total	Al	(wt%)
USY	0.125	0.148	0.273	47	14
2% Zn/USY	0.202	0.143	0.345	46.8	11
4% Zn/USY	0.237	0.129	0.366	47	6.3
6% Zn/USY	0.356	0.119	0.475	47.5	6.8
8% Zn/USY	0.355	0.114	0.469	47.7	—
2% Fe/USY	0.131	0.166	0.297	47	—
4% Fe/USY	0.155	0.178	0.333	46.5	14
6% Fe/USY	0.138	0.196	0.334	46.6	14

and increases in the numbers of weak and total acid sites in 2–8% Zn/USY catalysts, whereas the Fe/USY catalysts show increased total acidity and strong acidity. Thus the main difference between Zn/USY and Fe/USY catalysts is the change in the concentration of the strong acid sites.

3.3. Isopropylation of naphthalene over Zn-modified USY

The naphthalene isopropylation reactions were carried out over USY zeolites modified with various amounts of Zn (2–8%) oxide at 250 °C, 3.0 MPa and a WHSV of 3 h^{-1}. The naphthalene conversion, 2,6-DIPN selectivity and the 2,6/2,7-DIPN ratio are plotted against time on stream (TOS) in Fig. 6a. The Zn loadings of 4% and 6% improved naphthalene conversions to 94–95%, representing a significant increase from 86% over the parent USY. These two catalysts

Published on 07 October 2013. Downloaded by Memorial University of Newfoundland on 10/11/2013 16:34:56.

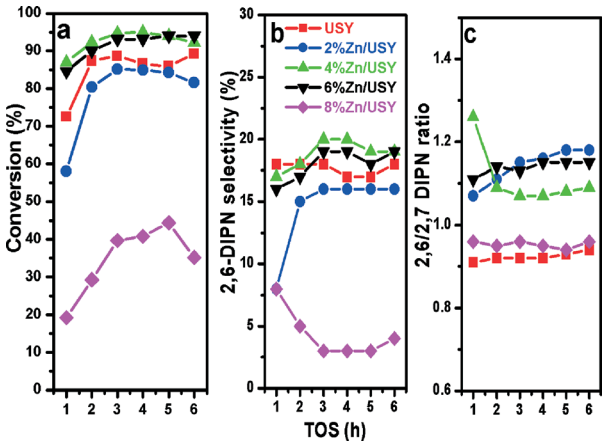

Fig. 6 Naphthalene conversion (a), 2,6-DIPN selectivity (b), and 2,6/2,7-DIPN ratio (c) against time on stream (TOS) for naphthalene isopropylation over Zn-modified USY catalysts. Reaction conditions: T = 250 °C; P = 30 bar; WHSV = 3 h^{-1}; isopropanol/naphthalene/decalin molar ratio: 1 : 2 : 7.5.

also exhibited excellent stability without any sign of deactivation for 6 h on stream.

The increased naphthalene conversion is accompanied by lower amounts of coke for Zn/USY. In general, coke formation is caused by side reactions such as cracking of the solvent, dehydration of isopropanol with subsequent oligomerization of propene, and cracking of oligomers.[36] The side reactions mostly occur on strong acid sites on the external surface, which tend to increase the coke formation at the pore entrance. The amount of coke deposited on the catalysts was measured by TPO analysis of the catalysts after isopropylation of naphthalene at 250 °C, 3.0 MPa, and a WHSV of 3 h^{-1} for 8 h, and the results are presented in Table 3 and Fig. 7.

The catalyst was flushed with a 10% O_2–He mixture at RT for 1 h, and then the temperature was raised to 750 °C at a rate of 8 °C min^{-1}.[37] In Fig. 7, the USY catalyst shows a peak in the range between 200 and 300 °C attributed to pre-adsorbed hydrocarbon species and the other peak at 600 °C attributed to the oxidation of deposited carbon species.[38,39]

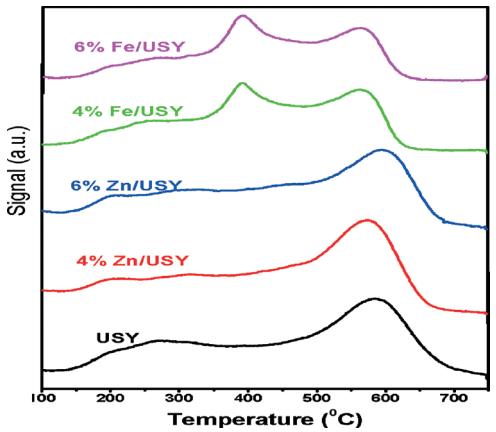

Fig. 7 TPO of used Zn- and Fe-loaded USY catalysts after isopropylation of naphthalene for 8 h.

Both 4% and 6% Zn/USY catalysts show decreased intensities of both peaks. Thus, the USY catalyst has a prevalent coke deposition of 14%, while the 4% and 6% Zn/USY catalysts show diminished amounts of coke (6.3% and 6.8%). The lower amounts of coke formation could be responsible for the higher conversion and improved stability of these Zn/USY catalysts. As mentioned already, the number of weak acidic sites increased, while the number of strong acidic sites decreased from the parent USY after the Zn loading (Table 3). These results are correlated with the ^{27}Al NMR results presented in Fig. 3. The ^{27}Al NMR spectrum of the parent USY showed a peak at 3 ppm corresponding to the octahedrally-coordinated extra framework Al species, which contribute to Lewis acid sites. The presence of these strong acid sites on the USY external surface can cause the formation of more coke. The intensity of the peaks at 3 ppm and 35 ppm decreased upon Zn loading, indicating a decrease in the number of strong acid sites on the USY external surface, which in turn would reduce coke formation.

The decreased number of strong acidic sites is responsible for the lower amount of coke formation.[36] It is well known that the optimum amount of acidic sites tends to prevent coke formation,[40–42] and our results reveal that a suitable admixture of both weak and strong acidic sites increases the activity with less coke formation. Over the 8% Zn/USY catalyst, conversion decreases to ~44% due to the blocking of pores by the larger amount of zinc oxide, which tends to restrict the diffusion of the reactant molecules. Hence the appearance of zinc oxide peak in XRD data indicates excessive pore blockage by large zinc oxide particles in the 8% Zn/USY catalyst.

The time profiles of 2,6-DIPN selectivity and the 2,6/2,7 ratio of Zn/USY catalysts are presented in Fig. 6b and c. The 2,6-DIPN selectivity and the 2,6-/2,7-DIPN ratio for the USY catalyst are 17% and 0.94, respectively. The 2,6-DIPN selectivity increases significantly to 20% over the 4% Zn/USY catalyst. But higher Zn loading decreases 2,6-DIPN selectivity all the way to 4% over the 8% Zn/USY catalyst. The shape selectivity ratio varies: 4% Zn/USY (1.18) > 6% Zn/USY (1.15) > 2% Zn/USY (1.09) > 8% Zn/USY ~USY (0.94). The result implies that 2–6% Zn loading decreases the pore size such that mild shape selectivity is exhibited. The ZnO species in these samples cannot be seen by XRD probably when they are in the form of very small particles or flat islands on the pore wall of USY. They provide a steric restriction to differentiate 2,6-DIPN molecules from 2,7-DIPN molecules. In contrast, large ZnO particles formed over the 8% Zn/USY catalyst only block the pore entrance and cannot improve the shape selectivity.

The products distributions in the naphthalene isopropylation reaction are plotted in Fig. 8. The parent USY catalyst shows IPN, DIPN and PIPN selectivities of 39%, 52% and ~6%, respectively. Over the Zn (2–6%)/USY catalysts, PIPN selectivity increased at the expense of IPN, while there were no considerable changes observed in the DIPN selectivity. This is in line with the increased naphthalene conversions on

This journal is © The Royal Society of Chemistry 2013

Published on 07 October 2013. Downloaded by Memorial University of Newfoundland on 10/11/2013 16:34:56.

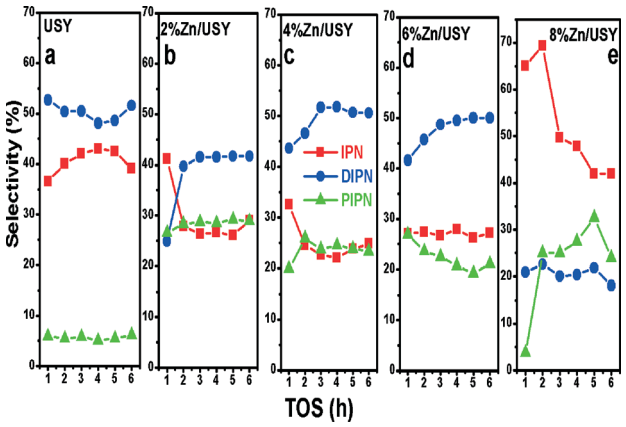

Fig. 8 Product distributions over Zn-modified USY catalysts; a: USY; b: 2% Zn/USY; c: 4% Zn/USY; d: 6% Zn/USY; e: 8% Zn/USY. Reaction conditions: T = 250 °C; P = 30 bar; WHSV = 3 h^{-1}; isopropanol/naphthalene/decalin molar ratio: 1 : 2 : 7.5.

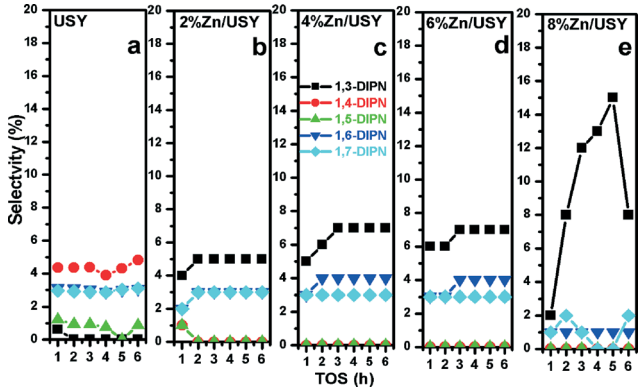

Fig. 9 DIPN isomer distributions for naphthalene isopropylation over Zn-modified USY catalysts; a: USY; b: 2% Zn/USY; c: 4% Zn/USY; d: 6% Zn/USY; e: 8% Zn/USY. Reaction conditions: T = 250 °C; P = 30 bar; WHSV = 3 h^{-1}; isopropanol/naphthalene/decalin molar ratio: 1 : 2 : 7.5.

these catalysts. In contrast, the Zn (8%)/USY catalyst showed a very high IPN selectivity of ~70% due to the pore blocking by the high Zn loading.

The isomeric distributions of DIPN (other than 2,6- and 2,7- DIPN) over the Zn-modified catalysts are presented in Fig. 9. Among the five minor isomers, 1,4-DIPN is obtained at the highest concentration of USY, whereas 1,3-DIPN and 1,6-DIPN are highest over the Zn-modified USY catalysts. 1,3-DIPN increased from 0.5% on USY to 15% on the 2–8% Zn/USY catalysts. Sugi *et al.* reported that the secondary isomerization of 1,6-DIPN and transalkylation of 1,3-DIPN lead to 2,6-DIPN.[10] Similarly in our case, we can assume that Zn (4, 6%) modification increases further isomerization of 1,6-DIPN and transalkylation of 1,3-DIPN toward more 2,6-DIPN. The above results indicate that the Zn-modified USY catalysts tend to favor smaller α,β (1,3 and 1,6-DIPN) isomers initially over larger α,α isomers (1,4 and 1,5-DIPN), which undergo further isomerization and transalkylation reactions to β,β isomers (2,6 and 2,7-DIPN). This provides further evidence of the shape selectivity effect induced by Zn loading and its pore restriction.

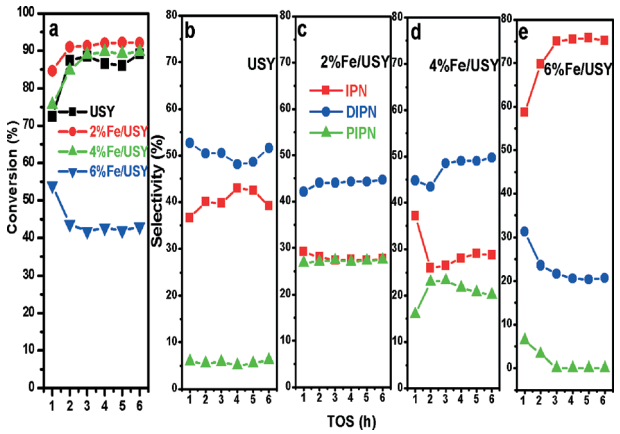

Fig. 10 Time profile of naphthalene conversion (a) and product distributions (b–e) for naphthalene isopropylation over Fe-modified USY catalysts; b: USY; c: 2% Fe/USY; d: 4% Fe/USY; e: 6% Fe/USY. Reaction conditions: T = 250 °C; P = 30 bar; WHSV = 3 h^{-1}; isopropanol/naphthalene/decalin molar ratio: 1 : 2 : 7.5.

3.4. Isopropylation of naphthalene over Fe-modified USY

The naphthalene isopropylation reactions were carried out using various amounts of Fe (2–6%) deposited on USY in the same reaction conditions. The conversion and product distributions are presented in Fig. 10 with time on stream. There is a slight improvement of naphthalene conversion over 2% and 4% Fe/USY catalysts from that over the parent USY. On the other hand, 6% Fe/USY catalyst shows much lower conversion and rapid deactivation. The deactivation is correlated with the presence of strong acidity. As presented in Table 3, the strong acidity increases from 0.148 mmol for the parent USY to 0.196 mmol for the 6% Fe/USY catalyst. The TPO analysis results show the peak between 300 and 400 °C attributed to the pre-adsorbed hydrocarbon species and the peak between 500 and 600 °C attributed to the oxidation of deposited carbon. The Fe-loaded USY catalysts showed a similar coke deposition to parent USY (14%) due to increased strong acidity.

The selectivity for 2,6-DIPN, the yield of 2,6-DIPN and the 2,6/2,7-DIPN ratio are presented in Fig. 11. Like Zn/USY, Fe

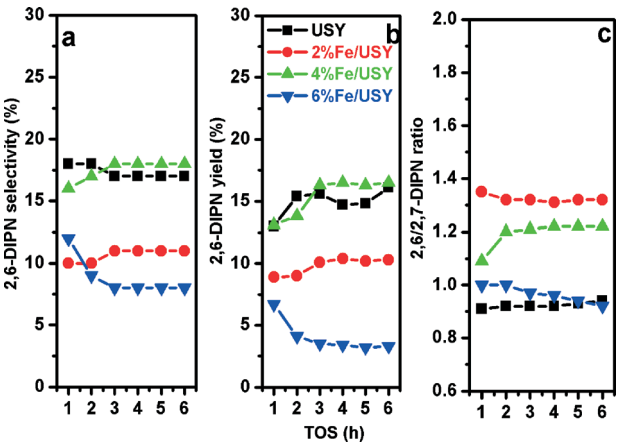

Fig. 11 2,6-DIPN selectivity (a), 2,6-DIPN yield (b), and 2,6/2,7-DIPN ratio (c) for naphthalene isopropylation over Fe-modified USY catalysts. Reaction conditions: T = 250 °C; P = 30 bar; WHSV = 3 h^{-1}; isopropanol/naphthalene/decalin molar ratio: 1 : 2 : 7.5.

Published on 07 October 2013. Downloaded by Memorial University of Newfoundland on 10/11/2013 16:34:56.

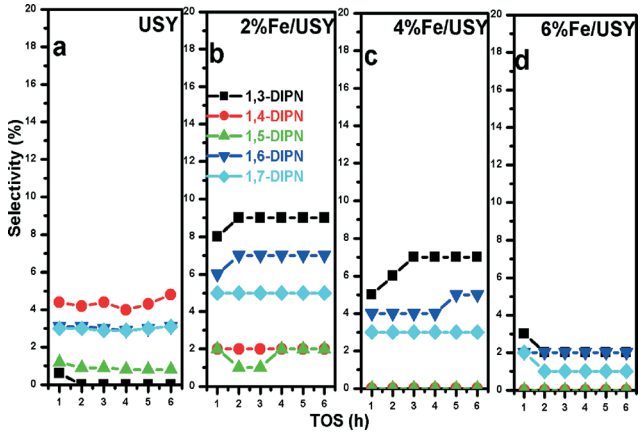

Fig. 12 The DIPN isomer distributions for naphthalene isopropylation over Fe-modified USY catalysts; a, USY; b, 2% Fe/USY; c, 4% Fe/USY; d, 6% Fe/USY. Reaction conditions: T = 250 °C; P = 30 bar; WHSV = 3 h^{-1}; isopropanol/naphthalene/decalin molar ratio: 1 : 2 : 7.5.

loading (2%, 4%) improves the production of DIPN and PIPN at the expense of IPN production. In contrast, the 6% Fe/USY catalyst shows reduced DIPN formation and negligible PIPN products, while IPN becomes the dominant product. All Fe-loaded USY catalysts show decreased selectivity for 2,6-DIPN, and thus only the 4% Fe/USY catalyst shows a slightly improved yield (~17%). The 2,6-/2,7-DIPN ratio increases significantly from 0.94 over the parent USY to 1.32 over the 2% and 4% Fe/USY catalysts. As in the case of Zn/USY, the significant increase in the 2,6/2,7-DIPN shape selectivity ratio is due to the decrease in pore size from 9.01 Å to 8.85 Å upon Fe loading on USY.

Thus loading suitable amounts (2% and 4%) of Fe on USY leads to the desired improvement in the performance of naphthalene isopropylation in terms of naphthalene conversion, 2,6-DIPN selectivity and 2,6/2,7 shape selectivity ratio. However, the effects on conversion and 2,6-DIPN selectivity are only marginal relative to Zn-loaded USY. This is correlated with the absence of any beneficial effect on coke formation and increased number of strong acid sites upon Fe loading compared to the parent USY. Thus FeO_x species can reduce the pore size of USY and bring shape selectivity.

The isomeric distributions of minor DIPN isomers over Fe/USY catalysts are presented in Fig. 12. As before, the 1,4-DIPN isomer is formed in the largest amount among these minor isomers over the parent USY, whereas the concentrations of 1,3- and 1,6- DIPN isomers increase dramatically over 2% and 4% Fe/USY catalysts. In contrast, the 1,3- and 1,6-DIPN selectivities decrease to very low values over the 6% Fe/USY catalyst. As mentioned, further isomerization of 1,6-DIPN and transalkylation of 1,3-DIPN would lead to 2,6-DIPN. Yet, the Fe loading on USY influences barely the further isomerization of 1,6-DIPN and transalkylation of 1,3-DIPN as the selectivity for 2,6-DIPN increases to a limited extent only over 4% Fe/USY.

4. Conclusions

The alkylation of naphthalene using isopropanol was carried out over commercial zeolites of MOR, BEA and USY. Their performance was consistent with their pore structures. Thus the large-pore USY zeolite showed high naphthalene conversion and good stability, but little shape selectivity. In contrast, small-pore MOR showed high shape selectivity, but low conversion and fast deactivation. The medium-pore BEA showed intermediate behaviour. To enhance the shape selectivity of USY, it was modified by zinc and iron oxides using the wet impregnation method. The modification not only enhanced the selectivity for 2,6-DIPN and the 2,6/2,7-DIPN shape selectivity ratio but also increased naphthalene conversion and catalyst stability. Zn loading was more effective than Fe loading. It appears that the small metal oxide islands are formed in the USY pores to decrease the pore size and thus render it shape selective. Zn loading also decreased the number of strong acidic sites responsible for the coke formation and increased the number of weak acid sites. The modified surface acid property improved naphthalene conversion and catalyst stability by reduced coke formation.

Acknowledgements

This work was supported by the Korean Ministry of Knowledge and Economy through the Research Institute of Industrial Science and Technology, Pohang.

Notes and references

1 D. Fraenkel, M. Cherniavsky, B. Ittah and M. Ievy, *J. Catal.*, 1986, **101**, 273.
2 G. Kamalakar, M. Ramakrishna Prasad, S. J. Kulkarni, S. Narayanan and K. V. Raghavan, *Microporous Mesoporous Mater.*, 2000, **38**, 135.
3 A. Katayama, M. Toba, G. Takeuchi, F. Mizukami, S. Niwa and S. Mitamura, *J. Chem. Soc., Chem. Commun.*, 1991, 39.
4 C. Song and S. Kirby, *Microporous Mater.*, 1994, **2**, 467.
5 J. H. Kim, Y. Sugi, T. Matsuzaki, T. Hanaoka, Y. Kubota, X. Tu and M. Matsumoto, *Microporous Mater.*, 1995, **5**, 113.
6 A. D. Schmitz and C. Song, *Catal. Lett.*, 1996, **40**, 59.
7 P. Moreau, A. Finiels, P. Geneste and J. Solofo, *J. Catal.*, 1992, **136**, 487.
8 P. Moreau, A. Finiels, P. Geneste, F. Moreau and J. Solofo, *Stud. Surf. Sci. Catal.*, 1993, **83**, 575.
9 W. Wei, W. Weiguo, O. V. Kikhtyanin, L. Lingfei, A. V. Toktarev, A. B. Ayupov, J. F. Khabibulin, G. V. Echevsky and H. Juan, *Appl. Catal., A*, 2010, **375**, 279–288.
10 Y. Sugi and M. Toba, *Catal. Today*, 1994, **19**, 319.
11 Y. Sugi, J. H. Kim, T. Matsuzaki, T. Hanaoka, Y. Kubota, X. Tu and M. Matsumoto, *Stud. Surf. Sci. Catal.*, 1994, **84**, 1837.
12 J. H. Kim, Y. Sugi, T. Matsuzaki, T. Hanaoka, Y. Kubota, X. Tu, M. Matsumoto, S. Nakata, A. Kato, G. Seo and C. Pak, *Appl. Catal., A*, 1995, **131**, 15.
13 A. D. Schmitz and C. Song, *Catal. Today*, 1996, **31**, 19.
14 S. Chu and Y. Chen, *Appl. Catal., A*, 1995, **123**, 51.
15 G. Kamalakar, S. J. Kulkarni, K. V. Raghavan, S. Unnikrishnan and A. B. Halgeri, *J. Mol. Catal. A: Chem.*, 1999, **149**, 283.

 This journal is © The Royal Society of Chemistry 2013

Published on 07 October 2013. Downloaded by Memorial University of Newfoundland on 10/11/2013 16:34:56.

16 P. Moreau, C. He, Z. Liu and F. Fajula, *J. Mol. Catal. A: Chem.*, 2001, **168**, 105.
17 G. Kamalakar, M. R. Prasad, S. J. Kulkarni and K. V. Raghavan, *Microporous Mesoporous Mater.*, 2002, **52**, 158.
18 S. W. Kang, O. Bong Yang and K. H. Lee, *Korean J. Chem. Eng.*, 1996, **34**, 400.
19 S. Hajimirzaee, G. A. Leeke and J. Wood, *Chem. Eng. J.*, 2012, **207–208**, 341.
20 R. Brzozowski and W. Skupiński, *J. Catal.*, 2002, **210**, 318.
21 C. Song and S. Kirby, *Prepr. Pap.-Am. Chem. Soc., Div. Petrol. Chem.*, 1993, **38**, 784.
22 J. Wang, P. Jung-Nam, P. Yong-Ki and C. W. Lee, *J. Catal.*, 2003, **220**, 272.
23 Y. Sugi, *J. Chin. Chem. Soc.*, 2010, **57**, 1.
24 R. Nagotkar, S. S. Khaire, S. Mayadevi and S. Sivasanker, *Indian J. Chem. Technol.*, 2004, **11**, 356.
25 R. Anand, R. Maheswari, K. U. Gore, S. S. Khaire and V. R. Chumbhale, *Appl. Catal., A*, 2003, **249**, 265.
26 B. M. Choudary, M. Sateesh, M. Lakshmi Kantam and K. V. Ram Prasad, *Appl. Catal., A*, 1998, **171**, 160.
27 L. Qian and Z.-F. Yan, *Colloids Surf., A*, 2001, **180**, 311.
28 M. Wark, H. Kessler and G. Schulz-Ekloff, *Microporous Mater.*, 1997, **8**, 253.
29 Z. Mingjin, Z. Anmin, D. Feng, Y. Yong and Y. Chaohui, *Sci. China, Ser. B: Chem.*, 2003, **46**, 223.
30 J. Rathousky, A. Zukal, N. Jaeger and G. Sschulz-Ekloff, *J. Chem. Soc., Faraday Trans.*, 1992, **88**, 489–495.
31 R. Shannon, *Acta Crystallogr., Sect. A: Cryst. Phys., Diffr., Theor. Gen. Crystallogr.*, 1976, **32**, 767.
32 H. Kosslick, H. Landmesser and R. J. Fricke, *J. Chem. Soc., Faraday Trans.*, 1997, **93**, 1849.
33 D. Esquivel, A. J. Cruz-Cabeza, C. Jimenez-Sanchidrian and F. J. Romero-Salguero, *Microporous Mesoporous Mater.*, 2011, **142**, 672.
34 P. Sun, S. Deore and A. Navrotsky, *Microporous Mesoporous Mater.*, 2007, **98**, 29.
35 H. Kosslick, G. Lischke, B. Parlitz, W. Storek and R. Fricke, *Appl. Catal., A*, 1999, **184**, 49.
36 I. Ferino, R. Monaci, E. Rombi, V. Solinas, P. Magnoux and M. Guisnet, *Appl. Catal., A*, 1999, **183**, 316.
37 A. Nieto-Márquez, J. C. Lazo, A. Romero and J. L. Valverde, *Chem. Eng. J.*, 2008, **144**, 530.
38 J. Strohm, J. Zheng and C. S. Song, *Prepr. Pap.-Am. Chem. Soc., Div. Petrol. Chem.*, 2003, **48**, 933.
39 J. Zheng, M. Guo and C. Song, *Fuel Process. Technol.*, 2008, **89**, 474.
40 G. Kamalakar, S. J. Kulkarni, K. V. Raghavan, S. Unnikrishnan and A. B. Halgeri, *J. Mol. Catal. A: Chem.*, 1999, **149**, 288.
41 S. J. Kulkarni, K. V. V. S. B. S. R. Murthy, K. Nagaiah, V. Sylesh Kumar, Y. V. Subba Rao, M. Subrahmanyam and A. V. Rama Rao, *Indian J. Chem. Technol.*, 1998, **5**, 62.
42 S. J. Kulkarni, K. V. V. S. B. S. R. Murthy, K. Nagaiah, M. Subrahmanyam and K. V. Raghavan, *Microporous Mesoporous Mater.*, 1998, **21**, 53.